

Depolarization in liquid-crystal televisions

J. Larry Pezzaniti, Stephen C. McClain, Russell A. Chipman, and Shih-Yau Lu

Department of Physics, Optics Building 318, University of Alabama in Huntsville, Huntsville, Alabama 35899

Received May 3, 1993

The depolarization of a TVT-6000 liquid-crystal television has been measured to vary between 2% and 9% as a function of bias voltage, angle of incidence, and incident polarization state.

Liquid-crystal televisions (LCTV's) are used not only as displays but also as spatial light modulators for filters in optical correlators and other optical information processing systems.^{1,2} Researchers showed that LCTV's are useful as phase modulators³⁻⁶ and polarization-state modulators.⁷

The polarization properties of LCTV's were investigated by several authors.^{4,5} In those investigations linearly polarized light that was aligned with the liquid-crystal molecular director was incident upon an LCTV, and the output polarization angle and ellipticity as a function of applied voltage were measured. Our research extends these investigations by measuring Mueller matrices of an LCTV, characterizing all its polarization forms. In addition to elliptical retardance (a combination of linear and circular retardance), the LCTV displays significant amounts of depolarization. Depolarization is the coupling of completely polarized light into partially polarized light.

The polarization properties of a TVT-6000 LCTV have been mapped as a function of bias voltage to the pixels and angle of incidence by a Mueller-matrix imaging polarimeter at 632.8 nm. When operated with the polarizers removed, the LCTV introduces between 2% and 9% depolarization, depending on the pixel bias voltage, the incident polarization state, and the angle of incidence. The device acts as an elliptical retarder whose magnitude and form are described.

Figure 1 displays maps of the fraction of unpolarized light F_U (depolarization) in the beams leaving the TVT-6000 LCTV for three incident polarization states at 632.8 nm. Each plot shows F_U as a function of angle of incidence and applied voltage. The gray scale addressing each pixel increases from zero across the bottom row, increasing linearly to 255 across the top row. The angle of incidence increases from -21° along the left column, through 0° up the middle (normal incidence), to 21° along the right column. The molecular director for the device is horizontal (parallel to the plane of incidence). The light leaving the LCTV is characterized by its Stokes vector $S = [S_0, S_1, S_2, S_3]^T$. The degree of polarization $DOP(S)$ of this beam is

$$DOP(S) = (S_1^2 + S_2^2 + S_3^2)^{1/2} / S_0, \quad (1)$$

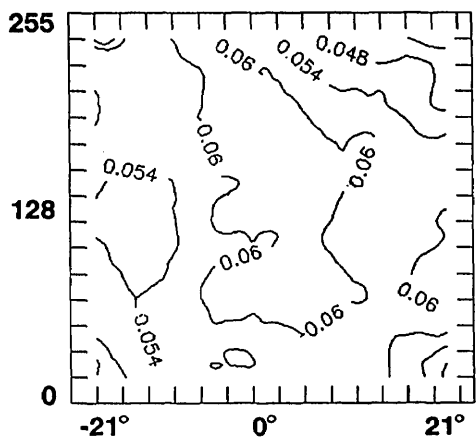
and the fraction of unpolarized light F_U , the quantity plotted in Fig. 1, is

$$F_U(S) = 1 - DOP(S). \quad (2)$$

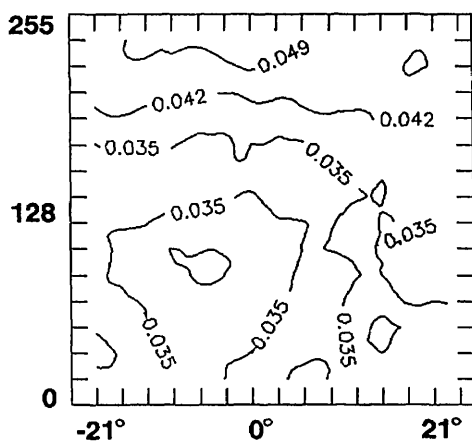
The data were smoothed with a 3×3 inverse-square weighted-average kernel. The average F_U over all incident polarization states and over the entire field is approximately 5.5%. F_U is smallest when vertically polarized light is incident. Left circular polarized light yields the largest depolarization. Significant variations with bias and angle of incidence are observed.

Figure 2 shows the Mueller-matrix imaging polarimeter developed at the University of Alabama in Huntsville.⁸ The instrument measures Mueller matrices in image form at 633 nm and at other visible and near-IR wavelengths. Mueller-matrix images can be acquired across the aperture of a sample, as in the measurements presented here, or in an image plane (polarization point-spread functions). A collimated 20-mm-diameter beam from a He-Ne laser passes through a fixed linear polarizer followed by a third-wave retarder whose orientation is varied. For these measurements a cylindrical lens generates a cylindrical wave that is incident upon the sample to permit simultaneous angle-of-incidence and bias measurements. A second cylindrical lens recollimates the light transmitted through the LCTV. The beam leaving the sample is analyzed by a third-wave retarder and a fixed linear polarizer. The irradiance distribution at the CCD is recorded for each incident and analyzed state. The CCD is a 512×512 pixel Photometrics, Inc., TH795B chilled scientific-grade detector with a 14-bit analog-to-digital converter.

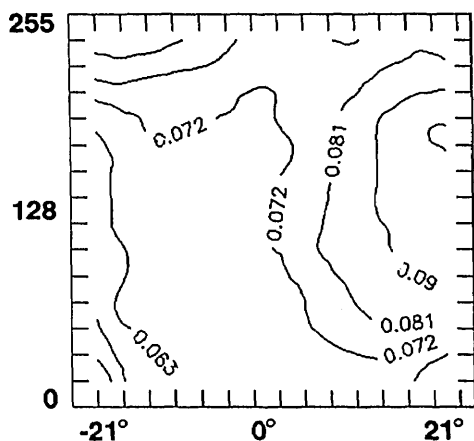
The LCTV was positioned such that the molecular director was aligned with the horizontal, and the electrodes addressing the device are on the side that the beam leaves. The ribbon cable comes out the top of the device. Positive angles of incidence are along counterclockwise rotations from the normal when viewed from the top. The optics collect a 0.1-N.A. beam from the LCTV and reimage the LCTV on the CCD. A set of 60 cylindrical waves with different polarization states is sequentially launched into the LCTV. In these measurements the center 256×256 pixels were imaged onto 32×32 CCD pixels. Between subsequent measurements the first retarder is rotated 6° and the second retarder is rotated 30° . From these 60 images, the Mueller matrices associated with the light path through each



(a)



(b)



(c)

Fig. 1. Fraction of transmitted light that is unpolarized for three incident polarizations: (a) horizontal, (b) 45°, (c) left circular. F_U is plotted as a function of angle of incidence (left to right) and applied voltage (bottom to top).

pixel are computed. The measured Mueller matrices for the LCTV are shown in Fig. 3. Extensive calibration procedures reduce systematic errors that are due to nonideal polarization components and drift.^{8,9}

Physical quantities, including retardance, depolarization, and diattenuation, are derived from a measured Mueller matrix. This device is intended to

perform as an electrically addressable retarder, and our measurements confirm that this is the dominant polarization effect. Specification of arbitrary elliptical retardance requires three degrees of freedom, for example, the magnitude, the orientation of the major axis, and the ellipticity. Alternatively, we can divide the elliptical retardance into the following components: δ_0 , the horizontal component; δ_{45} , the 45° component; and δ_R , the right circular component.

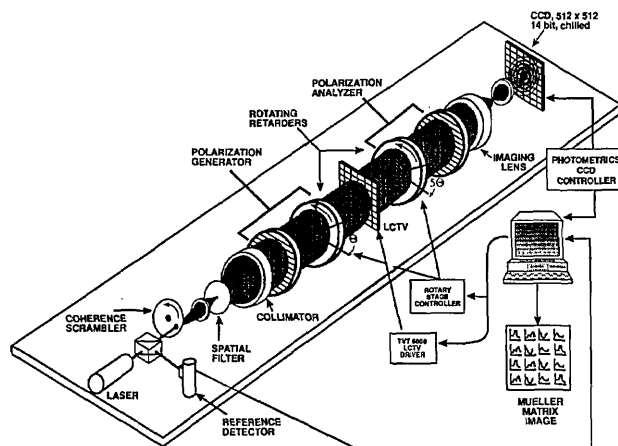


Fig. 2. Configuration of the Mueller-matrix imaging polarimeter. Utilizing rotating retarders and a 14-bit CCD camera, the polarimeter measures a series of 60 images to obtain a Mueller-matrix image. Accuracy is better than 1% at 632.8 nm. The instrument is entirely automated by a PC.

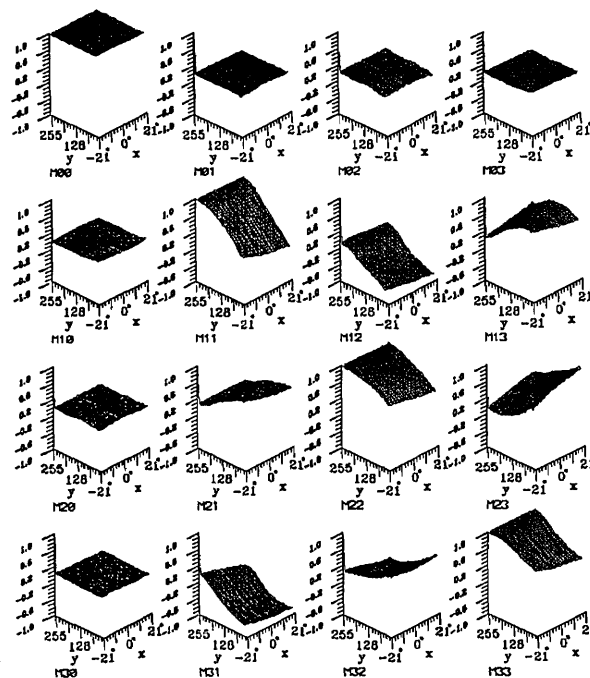


Fig. 3. Mueller-matrix images of the TVT-6000 LCTV as a function of angle of incidence and applied voltage. The Mueller matrices relate the input and output polarization states for arbitrary incident polarizations. These Mueller-matrix images contain the depolarization, retardance, and diattenuation and their variation over the field.

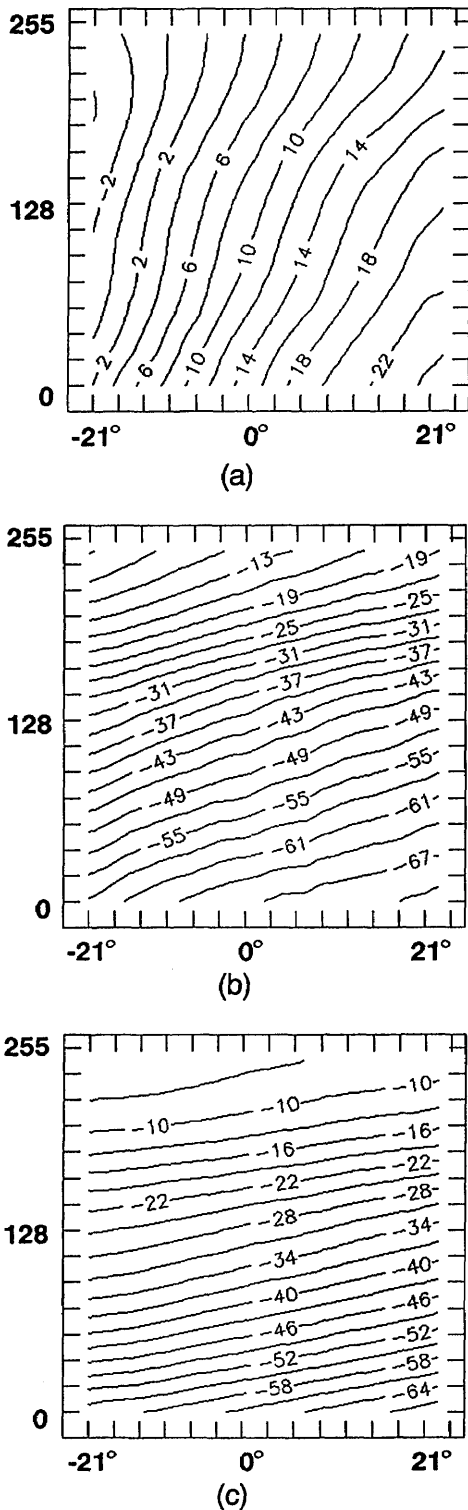


Fig. 4. Retardance of the LCTV as a function of angle of incidence and applied voltage: (a) horizontal component of linear retardance δ_0 , (b) 45° component of linear retardance δ_{45} , (c) circular retardance δ_R . The net retardance is elliptical, and its magnitude is nearly linear in applied voltage and angle of incidence.

The total retardance δ is then given by

$$\delta = (\delta_0^2 + \delta_{45}^2 + \delta_R^2)^{1/2}. \quad (3)$$

Figure 4 shows the retardance components as derived from the Mueller matrix.¹⁰ The retardance increases linearly with voltage and is weakly dependent on the angle of incidence. The retardance is of an elliptical form since $\delta_{45} \approx \delta_R$. Whereas a linear decrease in the magnitude of the retardance with applied voltage is evident in Fig. 4, the depolarization in Fig. 1 does not exhibit a similar linear dependence. This indicates that the source of the depolarization is not the same as the source of the polarization rotation. A significant part of the depolarization may result in part from scattering from the regions surrounding the LCTV pixels or from the edges of the pixels. Since this scattering may carry light out of the beam, the degree of polarization of the detected beam is expected to depend on the numerical aperture of the detection optics.

In conclusion, liquid crystal televisions exhibit significant amounts of depolarization in addition to their desired polarization effects. As much as 9% depolarization was observed in the TVT-6000. When the LCTV is used as a filter in an optical correlator, the unpolarized component will introduce noise at the Fourier-transform plane. Further investigations with the imaging polarimeter on LCTV's may quantify the effect of depolarization in various applications.

We acknowledge the support of the U.S. Air Force Office of Scientific Research and thank Jim Kirsch of the U.S. Army Missile Command for his assistance in this study. We also acknowledge helpful discussions with Don Gregory.

References

1. H. K. Lui, J. A. Davis, and R. A. Lilly, *Opt. Lett.* **10**, 635 (1985).
2. M. Young, *Appl. Opt.* **25**, 1024 (1986).
3. K. Lu and B. E. A. Saleh, *Appl. Opt.* **30**, 2354 (1991)
4. T. H. Barnes, T. E. Eiju, K. Matsuda, and N. Ooyama, *Appl. Opt.* **28**, 4845 (1989).
5. D. A. Gregory, J. A. Loudin, J. C. Kirsch, E. C. Tam, and F. T. S. Yu, *Appl. Opt.* **30**, 1374 (1991).
6. N. Konforti, E. Marom, and S. T. Wu, *Opt. Lett.* **13**, 251 (1988).
7. D. A. Gregory, *Appl. Opt.* **25**, 467 (1986).
8. J. L. Pezzaniti and R. A. Chipman, *Proc. Soc. Photo-Opt. Instrum. Eng.* **1317**, 280 (1990).
9. D. B. Chenault, J. L. Pezzaniti, and R. A. Chipman, *Proc. Soc. Photo-Opt. Instrum. Eng.* **1746**, 231 (1992).
10. S.-Y. Lu and R. A. Chipman, *Proc. Soc. Photo-Opt. Instrum. Eng.* **1746**, 197 (1992).